Austin Journal of Radiology

Open Access

Austin Publishing Group

Review Article

Peritoneal Metastases: Their Associated Imaging Features

Dromain C*
Service de Radiodiagnostic et Radiologie Interventionnelle, Bureau CIBM 09-084, rue Bugnon 46, 1011 Lausanne, Switzerland

***Corresponding author:** Clarisse Dromain, Service de Radiodiagnostic et Radiologie Interventionnelle, Bureau CIBM 09-084, rue Bugnon 46, 1011 Lausanne, Switzerland

Received: July 15, 2021; **Accepted:** August 31, 2021; **Published:** September 07, 2021

Abstract

Peritoneal Metastases (PM) detection remains a challenge even with modern imaging. Knowing imaging features of abnormal findings frequently associated with PM is of interest to improve PM detection. Although ascites is a common imaging finding of PM, the presence of ascites alone, even in patients with known cancer, is not enough to diagnose PM. The peritoneum should be read as an own organ with careful analysis of the ligament (e.g. falciform and hepatoduodenal ligament), the mesos and the omenta. Indirect manifestations of visceral peritoneal involvement is a segment of small bowel fixed to the parietal peritoneum, the appearance of blockage of free circulation of ascites, plurisegmental bowel obstruction and clumped bowel that is a strong predictor of diffuse involvement of the visceral peritoneum by a high grade tumor.

Ovarian and umbilical metastases are frequently associated with PM in particular in digestive cancers. Moreover, ovarian metastases has been shown to be less responsive to chemotherapy than other metastases and should not be chosen as a target lesion for RECIST assessment. The presence of cardiophrenic angle lymph nodes also increases the possibility of metastatic spread in peritoneum.

Finally, the most common PM mimickers include colonic diverticulum, mesenteric lymph nodes, splenosis implants, fat necrosis and postoperative changes after cytoreductive surgery and HIPEC.

Keywords: Peritoneal metastase; Peritoneal carcinomatosis; Imaging features; CT; MRI; PET-CT; Peritoneum

Introduction

Peritoneal metastases remain difficult to detect even with modern imaging. The peritoneal nodules are frequently of small size, the peritoneal cavity is vast including obscure locations. Furthermore, only few radiologists have developed expertise in assessment of this specific organ and systematic exploration and standardized documentation is rarely performed. The knowledge of indirect signs of peritoneal metastases as well as mimickers can help to improve diagnostic accuracy and patient management. The objective of this review is to present and describe the imaging features often associated with peritoneal metastases to assist the radiologist in his/her best efforts.

Ascites

Ascites from Peritoneal Metastases (PM) is due to altered vascular permeability, increased intraperitoneal protein concentration and obstructive lymphatic drainage [1]. Malignant ascites accounts for only 7-10% of all cases of ascites [2,3] suggesting that ascites is in most patients due to a benign condition such as cirrhosis, congestive heart failure, nephrosis, pancreatitis, or peritonitis and not a consequence of peritoneal malignant tumors [4]. Moreover, malignancy-related ascites in patients with known cancer can be due to different mechanisms including peritoneal metastases in 53% of cases but also due to massive liver metastases causing portal hypertension, budd-chiari syndrome due to malignancy occluding the hepatic vein [5], sinusoidal obstruction syndrome in particular in patient with colorectal cancer treated by oxaliplatine [6] (Figure 1), and due to bowel obstruction (Figure 2) [7].

In patients with peritoneal metastases, the presence of ascites is variable ranging from 20-70%. Malignant ascites is characterized by positive cytology in only 50-60% of patients, elevated protein concentrations and a low serum-ascites albumin gradient [2]. The origin of the primary tumor has an impact on the etiology and the quantity of ascites [8]: In ovarian and urinary bladder cancer, ascites

Figure 1: Ascites in a patient with a metastatic colic tumor. The ascites is due to extensive liver metastases from colon cancer with involvement of the medial and left hepatic veins.

Citation: Dromain C. Peritoneal Metastases: Their Associated Imaging Features. Austin J Radiol. 2021; 8(9): 1159.

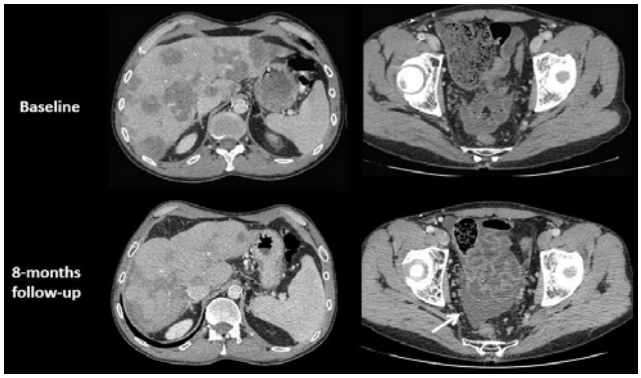

Figure 2: Patient with colon cancer and liver metastases treated with FOLFOX + bevacizumab. CT images performed 8 months after the start of the treatment show a discordance between a good response of liver metastases but the appearance of peritoneal fluid (arrow). The associated increase of the spleen volume is very suggestive of a sinusoidal obstruction syndrome, due to chemotherapy particularly oxaliplatin [6].

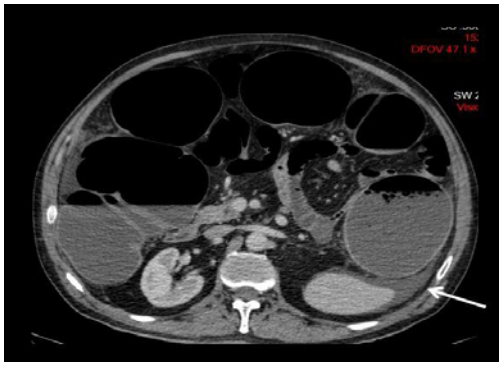

Figure 3: 55-year-old patient with a stenotic colic tumor. Transverse CT image shows a small amount of ascites (arrow). No peritoneal metastases was found during the surgery.

is the result of blockage of the draining lymphatic channels and of increased vascular permeability. In colonic, gastric, breast, pancreatic, and lung cancer, ascites is due to tumor cells producing fluid into the peritoneal cavity, due to obstruction/compression of the portal veins leading to portal hypertension, or due to liver failure. Lymphoma may cause lymph node obstruction with the accumulation of chylous ascites.

Presence of ascites can facilitate the detection of small peritoneal implants in patients with peritoneal metastases, in particular on the parietal peritoneum and in the pelvis (Figure 3).

Few imaging feature could help for characterizing ascites of unknown origin. As shown in Figure 4, ascites located in the lesser omental sac, in the hepatorenal pouch or associated with the tethered-bowel sign is more likely due to malignancy than of benign origin [9]. MRI with diffusion-weighted sequences may very helpful in case of small amount of fluid increasing the conspicuity of some tumor implants by the suppression of the SI of the ascites fluid. More recently, the use of a Hepatobiliary Phase (HBP) after Gd-BOPTA administration on MRI has been shown to be useful to distinguish benign from malignant ascites. Bonatti et al. correlated the degree of enhancement of peritoneal effusion during the HBP with their etiology and found that ascites enhancement is lower in-patient with peritoneal metastases than in patients with portal hypertension or hearth failure [10].

Take home message 1:

- The presence of ascites alone, even in a patient with known cancer, is not enough to diagnose PM.
- The presence of ascites in a patient with known cancer indicates the need for a careful analysis of the peritoneal cavity to look for other signs of potential PM.
- Ascites located in the lesser omental sac or in the hepatorenal pouch, and an associated tethered-bowel sign support a malignant etiology of the ascites.

Indirect Signs of PM

Imaging features suggesting tumoral involvement of the visceral peritoneum

Visceral peritoneal involvement remains a diagnostic challenge. To improve the detection of some peritoneal implants located in some tricky locations, it is required not only to look at the peritoneal cavity but also at the ligaments, the mesenteries and the omenta. In particular, the infiltration of the falciform or the hepato-duodenal ligament may be obvious but missed by non-dedicated radiologists (Figure 5).

Another manifestation of visceral peritoneal involvement is a segment of small bowel fixed to the parietal peritoneum, the appearance of blockage of free circulation of ascites, clumped bowel that is a strong predictor of diffuse involvement of the visceral peritoneum by a high-grade tumor and pluri-segmental bowel obstruction. With these findings, PM can be suspected even in the absence of a visible nodule or well-depicted thickening (Figure 6).

Figure 4. Transverse CT images of the abdomen and pelvis in a patient with ascites. Small tumor implants (arrows) are better depicted especially in the pelvis due to the presence of ascites.

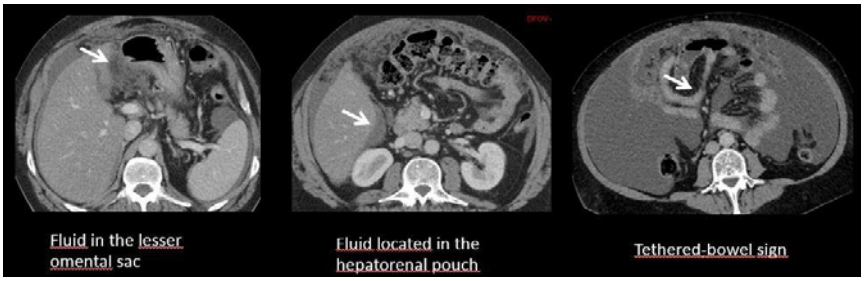

Figure 5: Malignant ascites. Ascites located in the lesser omental sac, in the hepatorenal pouch or associated with the tethered-bowel sign are highly suggestive to be malignant.

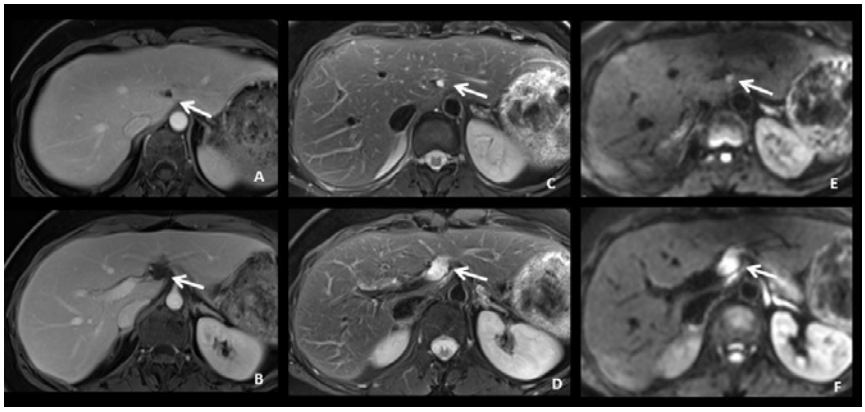

Figure 6: 44-year-old woman with mucinous colic cancer. MR images on T1W after Gd-based contrast agent administration (A-B), T2W (C-D) and DWI with b= 800 (E-F) show pseudocystic tumoral implant located in the falciform and the round ligaments (arrows). These peritoneal implants should not be misinterpreted as hepatic metastases or lymph nodes.

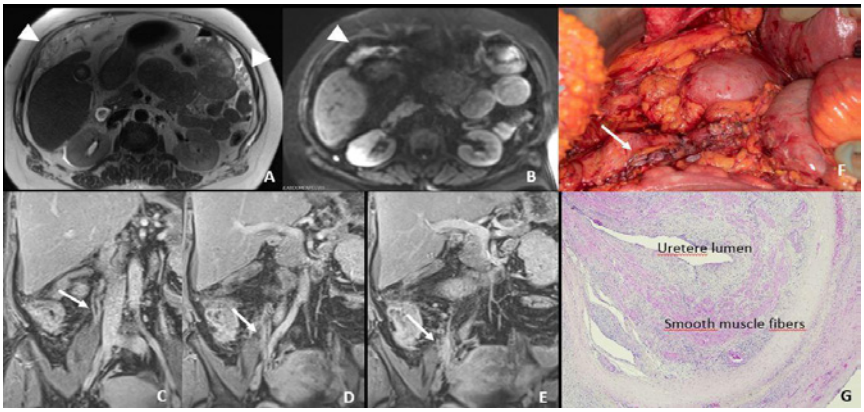

Figure 7: 41-year-old woman with peritoneal metastases from a caecal cancer. Transverse MR Images on T2W (A) and DW (B) show obvious peritoneal implants in the great omentum (arrowheads). Post-contrast T1W coronal images also well depicted a dilatation of the right ureter (arrow) with tissular involvement by peritoneal implant (E arrow). These peritoneal metastatic implants were remove during the surgery requiring a partial resection of the right ureter (F). Histopathological analysis confirmed a massive infiltration of ureter wall (G).

PET-CT or MRI diffusion-weighted images can help in these patients to detect additional findings and to increase the diagnostic accuracy.

Ureteral dilatation

Ureteral dilatation is another common indirect sign of PM (Figure 7). Appearance of a dilated ureter in the absence of an obvious stone is highly suggestive of PM in a patient known for digestive or ovarian cancer. The PET-CT is often of help showing a tracer uptake in the area of the obstruction (Figure 8). Peri-ureteral implants should not be misinterpreted as lymph node involvement.

Associated Imaging Features

Imaging features associated with PM correspond to abnormal findings frequently associated with PM. Their detection in a patient with a high risk of developing a PM must encourage a careful analysis of the entire peritoneal surface to increase detection of subtle implants.

Figure 8: 68-year-old man with metastatic colic cancer treated with surgery (primary tumor + liver metastases) after neo-adjuvant chemotherapy. CT images shows the appearance of a left ureteral dilatation with no obvious stone. FDG PET CT image shows a tracer uptake in the area of the ureteral stenosis highly suggestive of a peritoneal implant. This diagnosis was confirmed by surgery and pathology.

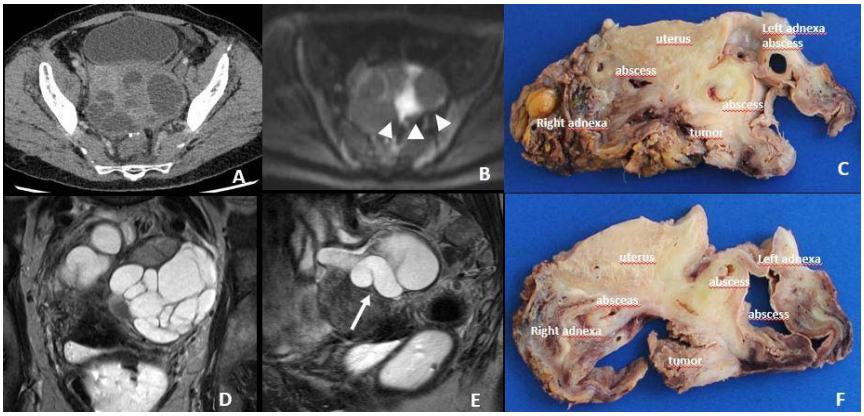

Figure 9: 65-year-old woman with a colic cancer resected 6 month ago. Transverse CT image reveals bilateral lobulating cystic masses in the adnexa suspicious for malignancy with possible diagnosis of ovarian metastases. Coronal (D) and sagittal (E) T2W MR Images show a tubular pattern (arrow) highly suggestive of a hydrosalpinx. The histopathological analysis (C, F) confirm the diagnosis of tubo-ovarian abscesses due to tumoral involvement of both fallopian tubes.

Ovarian metastases

Colorectal cancer is the most common non-gynecologic malignancy causing ovarian metastases with a rate of 1-10% for synchronous cancer and 1-2% for metachronous disease [11]. Ovarian metastases are frequently associated with additional peritoneal metastases. In the study of Goere et al. at least 52% of patients with PM of colorectal or appendiceal primary also have synchronous ovarian metastases [12]. Therefore, the presence of ovarian masses, in particular, large cystic masses on CT or MRI images in colorectal cancer should prompt careful analysis of the entire peritoneal cavity, including ligaments and mesenteries.

Ovarian metastases from colorectal cancer are often voluminous, cystic, mucinous and symptomatic. These ovarian metastases have been shown to be less responsive to systemic chemotherapy than extra-ovarian metastatic disease [12] (Figure 9). Consecutively, ovarian metastases should not be chosen as target lesions for assessment of treatment response to systemic chemotherapy. Moreover, resection of ovarian metastases should be discussed, even in the palliative setting, and is associated with a significantly prolonged survival in colorectal patients with ovarian metastases [13].

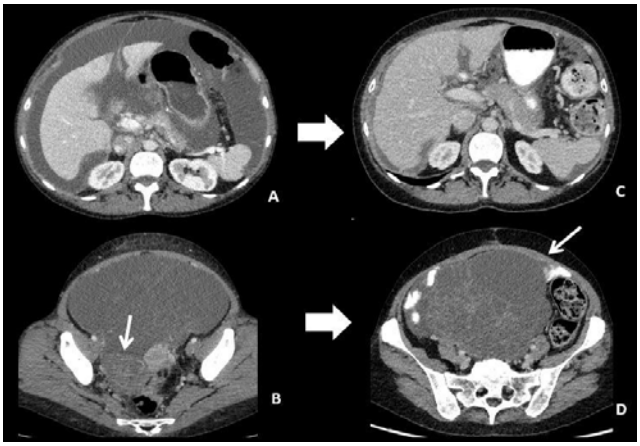

Figure 10: 45-year-old patient with right colon cancer. Transverse CT images of the initial staging (A-B) show synchronous ascites and a multicystic ovarian right mass. After treatment with folfiri, CT images (C-D) show a significant decrease of ascites and peritoneal implants but an important increase of the ovarian metastasis that has been shown to be less responsive to chemotherapy.

Umbilical metastases

Another associated clinical and radiologic feature is the Sister Mary Joseph nodule, a malignant metastatic umbilical nodule (Figure 10). The proposed route for the spread of cancer to the umbilicus includes direct extension from the peritoneum or spread via arteries, veins, and lymphatic channels or along the remnants of embryonic ligaments. A direct implantation after laparoscopy may also spread tumors to the umbilicus. It is most commonly found in association with adenocarcinoma and the most common primary sites are stomach, ovary, colon, and pancreas [14].

Cardiophrenic angle lymph node (CPALN)

The CPALN chain is a major lymph drainage system of both the

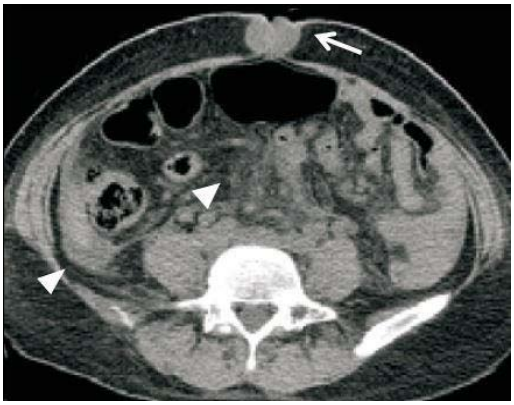

Figure 11: Transverse CT image shows a malignant metastatic nodule within the umbilicus. Also shown by the arrows head are ascites in the right paracolic sulcus and nodularity of the mesentery.

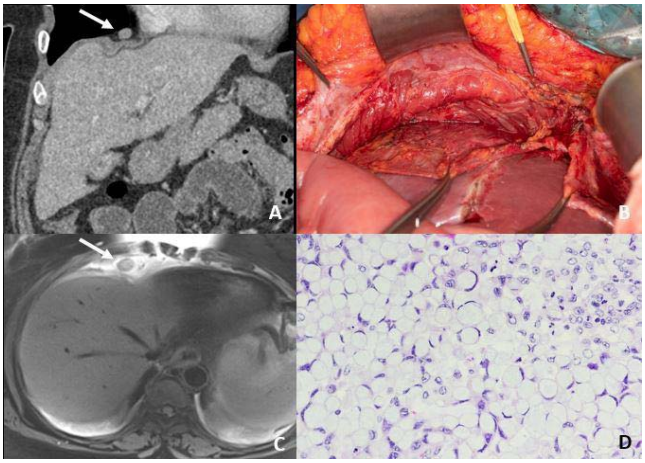

Figure 12: 41-year-old patient with peritoneal metastases from a colic cancer. CT images with coronal reconstruction (A) and transverse MR T2W image (C) show a cardiophrenic angle lymph node located above the diaphragm (arrow). This lymph node was surgically removed using a transabdominal dissection via incised diaphragm (B). The histopathological analysis of the surgical specimen (D) show a massive infiltration of the lymph node by the colic cancer that was a signet ring cell carcinoma.

peritoneum and the diaphragm and corresponds to lymph nodes located in an area adjacent to the pericardium within 2cm of the diaphragm [15-18] (Figure 11).

The association between CPALN and PM have been described in ovarian and colorectal cancer [19-20] (Figure 8). In advanced ovarian cancers CPLANs were found in 67% of patients by PET whereas only 33% were identified by CT. Patients with CPALN had significantly more ascites, higher CA-125 tumor marker levels, and more frequent peritoneal metastases compared to patients without CPALN. In colorectal cancer patients, a retrospective study, evaluated 550 consecutive patients with high-risk of PM [21]. CPALN was found in 45% of CT images and was significantly correlated with the presence of PM on multivariable analysis. The sensitivity for the detection of PM due to the presence of CPALN was 75% with a high negative predictive value of 86% suggesting that in absence of CPALN, PM can almost be excluded.

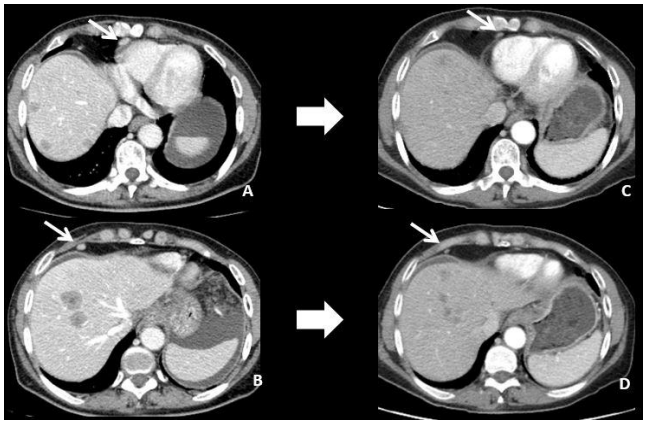

Figure 13: 56-year-old woman with liver and peritoneal metastases from a gastric cancer. Transverse CT images before (A-B) and after (C-D) chemotherapy using FOLFOX show a significant decrease in size of the liver metastasis and 2 CPALN (arrows) suggesting that these lymph nodes were malignant.

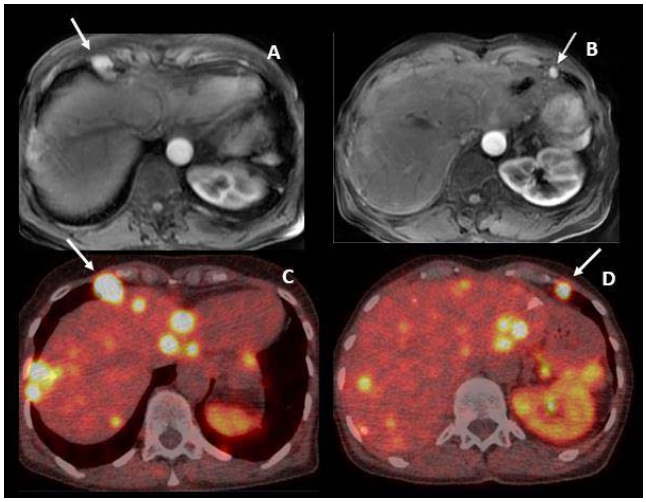

Figure 14: 44-year-old woman with metastatic neuroendocrine tumor from the small bowel and PM. T1 weighted MR images at the arterial phase after Gd-based contrast injection (A-B) shows 2 strongly enhancing cardiophrenic angle lymph nodes. These two CPALN also demonstrated an intense tracer uptake on F-DOPA PET-CT images (C-D).

Notwithstanding these findings, the association of CPLAN and peritoneal metastases remains controversial. On another consecutive cohort of 91 patients with low-risk of PM undergoing surgery for CRC, CPALN was detected in 39.5% of patients and no correlation was found between the presence of CPALN and the extent of PM [22] (Figure 12). The presence of distant metastases was associated with the presence of CPALN suggesting that CPALN is mainly an indicator of metastatic spread of colorectal cancer regardless of the location of the metastases. Moreover, the tumor infiltration of the CPALN is rarely proven, as most of these lymph nodes are not removed during surgery due to location above the diaphragm. Yoo et al. reported on 11 patients with ovarian cancer and peritoneal metastases undergoing cytoreductive surgery and systematic dissection of the CPALN >5mm an involvement by tumor in 45% of patients [23]. Finally, the prognostic impact of the presence of CPLAN in colorectal cancer

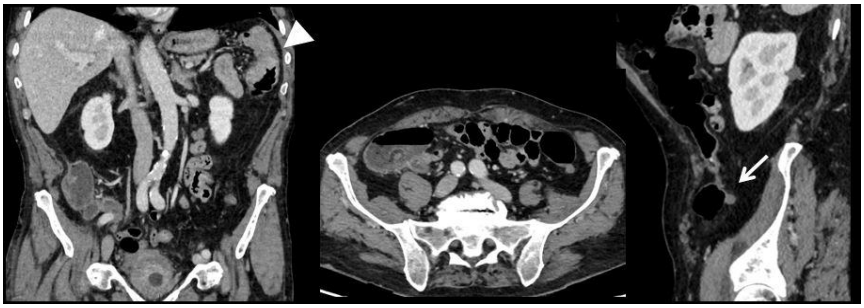

Figure 15: 68-year-old man with a colic cancer. Transverse CT image show a thickening of the left colic angle wall corresponding to the primary colic tumor (arrowhead) and a small pericolic nodule corresponding to a benign gas-free diverticulum (arrows).

patients has not been proven [21] (Figure 13).

Take home message 2:

- Visualization of indirect signs of peritoneal metastases such as ovarian metastases, CPALN, fixation and agglutination of small bowel requires a careful review of the entire peritoneal cavity, including folds and mesenteries.

- Ovarian metastases are frequently associated with PM from colon cancer. These metastases have been shown to be less responsive to chemotherapy than other sites of metastases and should never be chosen as target lesion for RECIST evaluation.

- The presence of CPALN in addition to other signs of PM should be clearly mentioned in the radiological report. The interest of additional investigation should be discussed during multidisciplinary tumor board meetings including MRI, PET-CT, laparoscopy, or close follow-up. Further studies are mandatory to better understand the prognostic significance of CPALN and the need, or not, to perform surgical removal.

Peritoneal Metastases Mimickers

There are a number of benign conditions that can be misinterpreted for peritoneal metastases. The most common are:

- A colonic diverticulum can be differentiated from tumor implant if it shows air filling (Figure 14).

- Mesenteric lymph node is tricky but most of the lymph nodes are close to the vessels and oval-shaped as compared to peritoneal implants which stick closer to the serosa of the bowel (Figure 15).

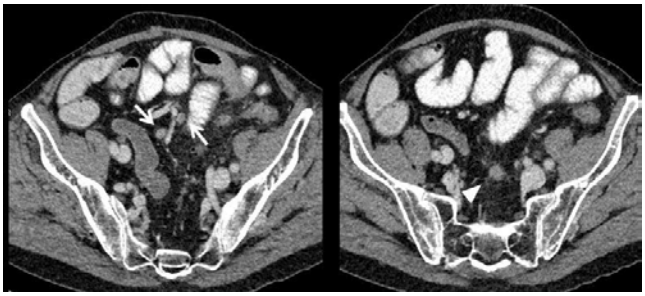

Figure 16: 64-year-old woman with peritoneal metastases from a colon cancer. Transverse CT images shows 2 oval-shape nodules located close to vessel in the mesosigmoïd corresponding to lymph nodes (arrows) and an ill-defined nodule also located in the mesosignoïd but away from vessels corresponding to a peritoneal implant (head of arrow).

- Splenosis implants (Figure 16). Assessment of the context (history of splenectomy or spleen trauma) and of the imaging features (nodules with similar signal than a normal spleen of all sequences and/or phases and in particular a marked enhancement during the arterial phase) will allow the correct diagnosis to be made. This entity is different from accessory spleen due to incorrect migration of nodules of splenic tissue during embryogenesis.

- Postoperative changes in patients previously treated by cytoreductive surgery and HIPEC. These post-operative changes could be depicted as perihepatic scalloping due to peritonectomy, fibrotic nodule (Figure 17). To distinguish a recurrent peritoneal implant from a post-operative changes it is crucial to have a baseline

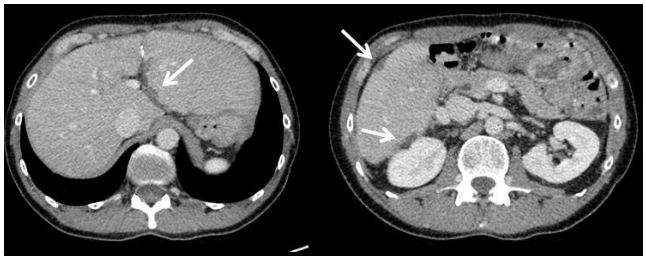

Figure 17: 38-year-old woman with peritoneal metastases from a colon cancer treated with cytoreudction surgery + HIPEC. The 2 months follow-up CT images show several areas of perihepatic scalopping (arrows) corresponding to post-operative changes due to perihepatic peritonectomies.

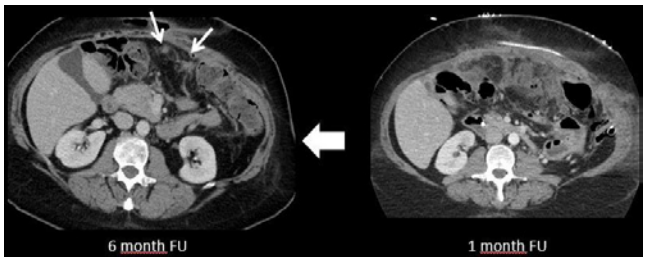

Figure 18: 64-year-old-woman with peritoneal metastases from a colon cancer treated with cytoreductive surgery and HIPEC. CT image performed 6 months after the surgery shows 2 peritoneal nodules (arrow) suspect for a recurrent peritoneal disease. However, the retrospective analysis of the CT performed 1 month after surgery shows an intra-abdominal abscess treated with percutaneous drainage suggesting post-operative changes.

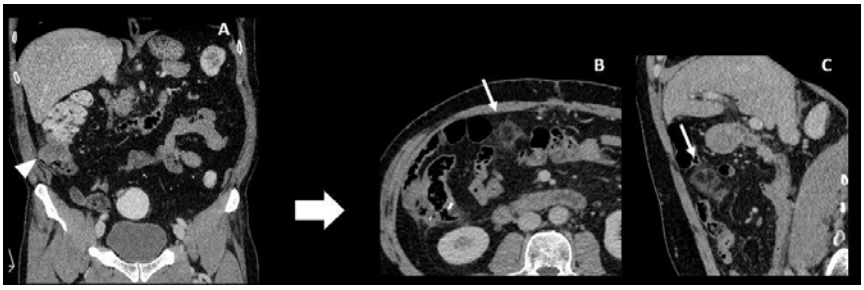

Figure 19: 71-year-old man with a colic cancer. Preoperative CT image (A) show an isolated caecal tumour (arrowhead) with no peritoneal metastases. On 3-months postoperative follow-up, CT images (B-C) show a round fatty encapsulated mass of the great omentum highly suggestive of an omental infarction.

postoperative CT about 2 months after surgery to be able to depict postoperative changes and then to follow the patient (Figure 18).

- Fat necrosis include torsion of an epiploic appendix, infraction of the great omentum and fat necrosis related to trauma and pancreatitis [24]. Omental infarction may occur after a surgical trauma and should not be misinterpreted as a peritoneal recurrence after surgery of the primary tumor or after cytoreduction surgery and HIPEC. Its diagnosis is based on the location, on the surgical site and it appearance as a fatty encapsulated mass (Figure 19).

Take home message 3:

- A 1-2 months post-operative CT is needed after cytoreduction surgery + HIPEC in order to correctly diagnose post-operative changes from peritoneal recurrent disease.

References

1. Tamsma JT, Keizer HJ, Meinders AE. Pathogenesis of malignant ascites: Starling's law of capillary hemodynamics revisited. Annals of oncology: official journal of the European Society for Medical Oncology. 2001; 12: 1353-1357.
2. Sangisetty SL, Miner TJ. Malignant ascites: A review of prognostic factors, pathophysiology and therapeutic measures. World journal of gastrointestinal surgery. 2012; 4: 87-95.
3. Becker G, Galandi D, Blum HE. Malignant ascites: systematic review and guideline for treatment. Eur J Cancer. 2006; 42: 589-597.
4. Huang LL, Xia HH, Zhu SL. Ascitic Fluid Analysis in the Differential Diagnosis of Ascites: Focus on Cirrhotic Ascites. Journal of clinical and translational hepatology. 2014; 2: 58-64.
5. Runyon BA. Malignancy-related ascites and ascitic fluid "humoral tests of malignancy". Journal of clinical gastroenterology. 1994; 18: 94-98.
6. Valla DC, Cazals-Hatem D. Sinusoidal obstruction syndrome. Clinics and research in hepatology and gastroenterology. 2016; 40: 378-385.
7. O'Daly BJ, Ridgway PF, Keenan N, Sweeney KJ, Brophy DP, Hill AD, et al. Detected peritoneal fluid in small bowel obstruction is associated with the need for surgical intervention. Canadian journal of surgery Journal canadien de chirurgie. 2009; 52: 201-206.
8. Runyon BA, Hoefs JC, Morgan TR. Ascitic fluid analysis in malignancy-related ascites. Hepatology (Baltimore, Md). 1988; 8: 1104-1109.
9. Seltzer SE. Analysis of the tethered-bowel sign on abdominal CT as a predictor of malignant ascites. Gastrointestinal radiology. 1987; 12: 245-249.
10. Bonatti M, Valletta R, Zamboni GA, Lombardo F, Senoner M, Simioni M, et al. Ascites relative enhancement during hepatobiliary phase after Gd-BOPTA administration: a new promising tool for characterizing abdominal free fluid of unknown origin. Eur Radiol. 2019.
11. Koves I, Vamosi-Nagy I, Besznyak I. Ovarian metastases of colorectal tumours. European journal of surgical oncology: the journal of the European Society of Surgical Oncology and the British Association of Surgical Oncology. 1993; 19: 633-635.
12. Goere D, Daveau C, Elias D, Boige V, Tomasic G, Bonnet S, et al. The differential response to chemotherapy of ovarian metastases from colorectal carcinoma. European journal of surgical oncology: the journal of the European Society of Surgical Oncology and the British Association of Surgical Oncology. 2008; 34: 1335-1339.
13. Lee SJ, Lee J, Lim HY, Kang WK, Choi CH, Lee JW, et al. Survival benefit from ovarian metastatectomy in colorectal cancer patients with ovarian metastasis: a retrospective analysis. Cancer chemotherapy and pharmacology. 2010; 66: 229-235.
14. Chalya PL, Mabula JB, Rambau PF, McHembe MD. Sister Mary Joseph's nodule at a University teaching hospital in northwestern Tanzania: a retrospective review of 34 cases. World journal of surgical oncology. 2013; 11: 151.
15. Glazer HS, Aronberg DJ, Sagel SS, Friedman PJ. CT demonstration of calcified mediastinal lymph nodes: a guide to the new ATS classification. AJR American journal of roentgenology. 1986; 147: 17-20.
16. Shibata S, Yamaguchi S, Kaseda M, Ichihara N, Hayakawa T, Asari M. The time course of lymphatic routes emanating from the peritoneal cavity in rats. Anatomia, histologia, embryologia. 2007; 36: 78-82.
17. Souilamas R, Hidden G, Riquet M. Mediastinal lymphatic efferents from the diaphragm. Surgical and radiologic anatomy: SRA. 2001; 23: 159-162.
18. Parungo CP, Soybel DI, Colson YL, Kim SW, Ohnishi S, DeGrand AM, et al. Lymphatic drainage of the peritoneal space: a pattern dependent on bowel lymphatics. Annals of surgical oncology. 2007; 14: 286-298.
19. Hynninen J, Auranen A, Carpen O, Dean K, Seppanen M, Kemppainen J, et al. FDG PET/CT in staging of advanced epithelial ovarian cancer: frequency of supradiaphragmatic lymph node metastasis challenges the traditional pattern of disease spread. Gynecol Oncol. 2012; 126: 64-68.
20. Caramella C, Pottier E, Borget I, Malka D, Goere D, Boige V, et al. Value of cardiophrenic angle lymph node for the diagnosis of colorectal peritoneal carcinomatosis. Eur J Cancer. 2013; 49: 3798-3805.
21. Elias D, Borget I, Farron M, Dromain C, Ducreux M, Goere D, et al. Prognostic significance of visible cardiophrenic angle lymph nodes in the presence of peritoneal metastases from colorectal cancers. European journal of surgical oncology: the journal of the European Society of Surgical Oncology and the British Association of Surgical Oncology. 2013; 39: 1214-1218.
22. Jeune F, Brouquet A, Caramella C, Gayet M, Abdalla S, Verin AL, et al. Cardiophrenic angle lymph node is an indicator of metastatic spread but not specifically peritoneal carcinomatosis in colorectal cancer patients: Results of a prospective validation study in 91 patients. European journal of surgical oncology: the journal of the European Society of Surgical Oncology and the British Association of Surgical Oncology. 2016; 42: 861-868.
23. Yoo HJ, Lim MC, Song YJ, Jung YS, Kim SH, Yoo CW, et al. Transabdominal cardiophrenic lymph node dissection (CPLND) via incised diaphragm replace conventional video-assisted thoracic surgery for cytoreductive surgery in advanced ovarian cancer. Gynecol Oncol. 2013; 129: 341-345.

24. Kamaya A, Federle MP, Desser TS. Imaging manifestations of abdominal fat necrosis and its mimics. Radiographics: a review publication of the Radiological Society of North America, Inc. 2011; 31: 2021-2034.